J|A|C|S ARTICLES

Published on Web 06/16/2009

Universal Translators for Nucleic Acid Diagnosis

John M. Picuri, Brian M. Frezza, and M. Reza Ghadiri*

Departments of Chemistry and Molecular Biology and Skaggs Institute for Chemical Biology, The Scripps Research Institute, 10550 North Torrey Pines Road, La Jolla, California 92037

Received March 28, 2009; E-mail: ghadiri@scripps.edu

Abstract: Defined broadly, molecular translators are constructs that can convert any designated molecular input into a unique output molecule. In particular, the development of universal nucleic acid translators would be of significant practical value in view of the expanding biomedical importance of gene diagnostics. Currently, diagnostic assays for nucleic acids must be individually developed and optimized for each new sequence because inputs for one assay are sequence-specific and are therefore incompatible with any other assay designed for the detection of a different nucleic acid. However, if a desired nucleic acid sequence could be translated *in vitro* into a predetermined nucleic acid output for which there is already a known diagnostic assay, then that single assay could be easily adapted to detect nearly any strand. Here we investigate PCR-independent isothermal molecular translation strategies that function without the need for post-translation purification and can be implemented with commercially available components. Translation yields up to 96% are obtained in 5 min at room temperature with minimal background reaction (<1%) and with discrimination of single nucleotide polymorphisms in the input sequence. Furthermore, we apply these translators to adapt a high-gain HIV diagnostic system for high-throughput detection of hepatitis C, avian influenza (H5N1), and smallpox without making changes to the underlying assay. Finally, we show the feasibility of translating small-molecule interactions into nucleic acid outputs by demonstrating the utility of a DNA aptamer for translating adenosine into a readily detectable output DNA sequence. Additionally, equilibrium expressions are described in order to facilitate rational engineering of aptameric translators for label-free detection of any molecule that an aptamer can recognize.

Introduction

Living cells employ complex machineries and pathways to translate genetic information into molecular instructions. By analogy, an ability to chemically translate any input molecular information into a readily processed output would be invaluable for rational engineering of advanced biomedical and diagnostic systems. Nucleic acids are particularly well-suited for such molecular translation and diagnostics applications as a result of their predictable sequence-specific hybridization properties, ease of preparation *in vitro* using chemical synthesis or *in vivo* using the tools of molecular biology, and numerous functions in biology. In this context, a simple PCR-independent isothermal strategy for converting any input nucleic acid sequence into any other output nucleic acid sequence of interest would not only extend the generality of sequence-specific nucleic acid detection methods[1] but also allow modular interfacing between diverse DNA nanotechnologies such as 2D and 3D nanoarchitectures,[2] molecular machines,[3] DNA templated reactivity,[4] and molecular computers.[5]

Traditionally, nucleic acid translators have consisted of ligation-based systems[6] where the input DNA directs the ligation of smaller fragments to produce a full-length output. More recently, a strategy based on restriction enzyme activity has also been investigated.[7] While these systems perform the fundamental task of translation, they often suffer from key experimental shortcomings that can greatly limit their practical applications, including modest translation yields, slow reaction kinetics, high background reactivity, and complex component architectures. Perhaps most importantly, though, these strategies require post-translation purification to obtain single-stranded output in isolation before the results may be coupled to further assays.

Herein, we present an in-depth study that characterizes the scope and limitations of two new classes of universal nucleic

(1) (a) Schweitzer, B.; Kingsmore, S. *Curr. Opin. Biotechnol.* **2001**, *12*, 21–27. (b) Rosi, N. L.; Mirkin, C. A. *Chem. Rev.* **2005**, *105*, 1547–1562.

(2) (a) Seeman, N. C. *Curr. Opin. Struct. Biol.* **1996**, *6*, 519–526. (b) Winfree, E.; Liu, F.; Wenzler, L. A.; Seeman, N. C. *Nature* **1998**, *394*, 539–544. (c) Seeman, N. C. *Nature* **2003**, *421*, 427–431. (d) Shih, W. M.; Quispe, J. D.; Joyce, G. F. *Nature* **2004**, *427*, 618–621. (e) Chworos, A.; Severcan, I.; Koyfman, A. Y.; Weinkam, P.; Oroudjev, E.; Hansma, H. G.; Jaeger, L. *Science* **2004**, *306*, 2068–2072. (f) Rothemund, P. W. *Nature* **2006**, *440*, 297–302.

(3) (a) Yurke, B.; Turberfield, A. J.; Mills, A. P., Jr.; Simmel, F. C.; Neumann, J. L. *Nature* **2000**, *406*, 605–608. (b) Yan, H.; Zhang, X.; Shen, Z.; Seeman, N. C. *Nature* **2002**, *415*, 62–65. (c) Simmel, F. C.; Dittmer, W. U. *Small* **2005**, *1*, 284–299.

(4) (a) Bohler, C.; Nielsen, P. E.; Orgel, L. E. *Nature* **1995**, *376*, 578–581. (b) Kanan, M. W.; Rozenman, M. M.; Sakurai, K.; Snyder, T. M.; Liu, D. R. *Nature* **2004**, *431*, 545–549. (c) Li, X.; Liu, D. R. *Angew. Chem., Int. Ed.* **2004**, *43*, 4848–4870. (d) Sakurai, K.; Snyder, T. M.; Liu, D. R. *J. Am. Chem. Soc.* **2005**, *127*, 1660–1661. (e) Silverman, A. P.; Kool, E. T. *Chem. Rev.* **2006**, *106*, 3775–3789. (f) Grossmann, T. N.; Strohbach, A.; Seitz, O. *ChemBioChem* **2008**, *9*, 2185–2192.

(5) (a) Adleman, L. M. *Science* **1994**, *266*, 1021–1024. (b) Lipton, R. J. *Science* **1995**, *268*, 542–545. (c) Ouyang, Q.; Kaplan, P. D.; Liu, S.; Libchaber, A. *Science* **1997**, *278*, 446–449. (d) Liu, Q.; Wang, L.; Frutos, A. G.; Condon, A. E.; Corn, R. M.; Condon, A. E. *Nature* **2000**, *403*, 175–179. (e) Landweber, L. F.; Lipton, R. J. *Lect. Notes Comput. Sci.* **1997**, *1256*, 56–64.

10.1021/ja902490x CCC: $40.75

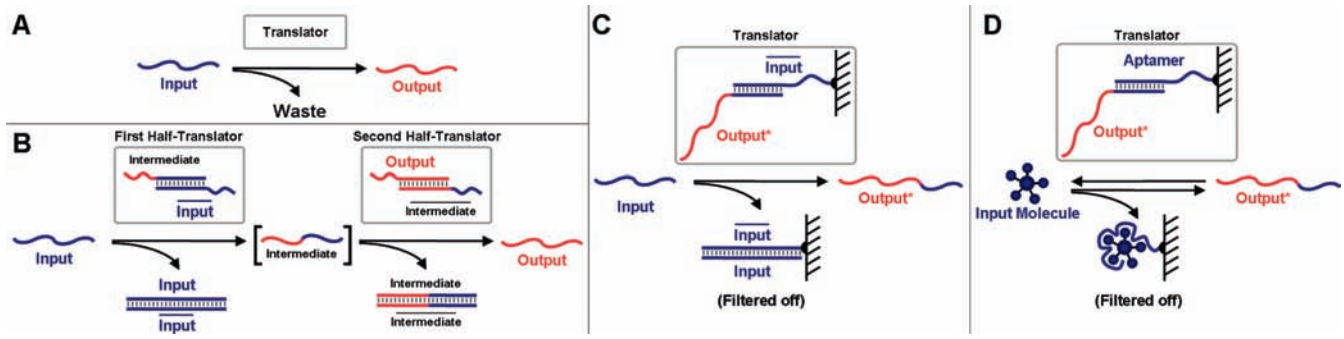

Figure 1. Displacement-based universal translation. (A) A universal translator (gray box) must effectively convert one input sequence (blue) into a completely unique output sequence (red) in a programmable fashion. Sequences should be translated in a dose-dependent manner to preserve quantitative information. (B) Toe-hold sequestered translation. Toe-hold sequestering is a method of enforcing conditional displacement by requiring a primary displacement event to expose a single-stranded toe-hold (which is initially sequestered in a stable duplex) before that toe-hold can be utilized in a secondary displacement event. In the example shown, the output sequence cannot be displaced from the output−intermediate duplex until the intermediate's toe-hold is made available in single-stranded form via displacement from the intermediate−input duplex by the input strand. Two translator duplexes are needed to translate between fixed input and output sequences, because each translation must contain at least a toe-hold from the previous input. (C) Solid-phase translation. Biotin-conjugated (black semicircles) DNA is immobilized on streptavidin Sepharose (black hash marks). In a solid-phase translation, the input sequence (blue) simply releases the output sequence (red-blue) via displacement from the solid phase into solution. After filtering, this will leave only output displaced by the input in solution. For the most part, the anchor that holds the output to the immobilized strand (denoted with an asterisk) has little effect on further assays. However, if a strict conversion with no trailing sequences is required, two translators can be coupled in series much the same way the toe-hold sequestering method requires. (D) Aptamer-assisted solid-phase molecular translation. Molecular inputs (represented nonspecifically by the abstract shape) can be translated to output sequences through the use of SELEX[12,13,24]-generated aptamers. Aptamer sequences selected for their ability to bind molecular targets are first immobilized to a solid support. Next, the immobilized aptamer is annealed to an output strand (red-blue) that contains a short segment complementary to the aptamer (blue) appended to the output sequence (red). The aptamer competitively binds both the output sequence and the molecular input. Thus, after addition of the input molecule, a new equilibrium is established and some of the output sequence is displaced into solution. After filtration, this leads to a dose-dependent exchange of output sequence for input molecules.

acid translators originating from recent advances in DNA logic gating.[8,9] Both approaches utilize sequence-directed DNA strand displacement as the underlying mechanism of translation (Supporting Information, Figure S1). In this process, DNA can bind to exposed single-stranded "toe-hold" regions of complementary strands and irreversibly displace a shorter strand via a three-way branch migration mechanism.[10] Here we describe simple constructs that efficiently translate several different biologically relevant input sequences (indicative of the hepatitis C virus, avian influenza (H5N1), or smallpox virus infection) into a unique output in 5 min at room temperature without the need for a separate purification step. In addition, we assess the selectivity of the translator in terms of the ability to discriminate single nucleotide polymorphisms in the input sequence. Furthermore, to demonstrate their practical application, we use these translators to allow for high-throughput adaptation of a highly sensitive DNA-detecting technology previously designed to detect only HIV diagnostic sequences.[11] Finally, we investigate extending the range of inputs to virtually any protein or small molecule through the use of a SELEX[12,13]-generated aptamer-assisted translation strategy.

The first of the two nucleic acid translation strategies investigated, known as toe-hold sequestering[8,14,15] (Figure 1B), is an effective method of enforcing conditional DNA strand displacement by requiring a primary displacement event to expose a single-stranded toe-hold before that toe-hold can be utilized in a secondary displacement. A complete translation between two unrelated sequences can be implemented by coupling two half-translations, each of them toe-hold sequestered. The first half-translator requires the input sequence to bind and displace a sequestered intermediate, which can then subsequently bind to and displace the output on the second half-translator (Figure 1B).

The second style of translation investigated is termed solid-phase translation[9] (Figure 1C). In this system, output DNA is appended to a small fragment of the input sequence and then annealed to an immobilized full complement to the input sequence. When the input sequence is present, it displaces the duplex anchoring the output to the solid support, thus releasing the output into solution (Figure 1C). After filtering the beads, only output DNA produced by the translation will be left in solution. As an extension of this approach, we also introduce an aptamer-assisted solid-phase translation strategy capable of translating aptameric binding of an input molecule into output DNA (Figure 1D). In this design, an immobilized aptamer competes for binding to the input molecule or to the output sequence. Any input molecule that competitively binds the aptamer therefore removes the anchor between the output sequence and the solid support, leaving the output free in solution. After filtering, this results in a dose-dependent translation of the input molecule into output DNA. Because RNA or DNA aptamers can be evolved or selected to bind a wide variety of proteins,[13] small molecules,[12] and even unknown phenotypic

(6) (a) Liao, S.; Seeman, N. C. *Science* **2004**, *306*, 2072–2074. (b) Endo, M.; Uegaki, S.; Majima, T. *Chem. Commun.* **2005**, 3153–3155. (c) Tabor, J. J.; Levy, M.; Ellington, A. D. *Nucleic Acids Res.* **2006**, *34*, 2166–2172. (d) Garibotti, A. V.; Liao, S.; Seeman, N. C. *Nano Lett.* **2007**, *7*, 480–483.
(7) Beyer, S.; Simmel, F. C. *Nucleic Acids Res.* **2006**, *34*, 1581–1587.
(8) Seelig, G.; Soloveichik, D.; Zhang, D. Y.; Winfree, E. *Science* **2006**, *314*, 1585–1588.
(9) Frezza, B. M.; Cockroft, S. L.; Ghadiri, M. R. *J. Am. Chem. Soc.* **2007**, *129*, 14875–14879.
(10) Reynaldo, L. P.; Vologodskii, A. V.; Neri, B. P.; Lyamichev, V. I. *J. Mol. Biol.* **2000**, *297*, 511–520.
(11) (a) Saghatelian, A.; Guckian, K. M.; Thayer, D. A.; Ghadiri, M. R. *J. Am. Chem. Soc.* **2003**, *125*, 344–345. (b) Gianneschi, N. C.; Ghadiri, M. R. *Angew. Chem., Int. Ed.* **2007**, *46*, 3955–3958.
(12) Ellington, A. D.; Szostak, J. W. *Nature* **1990**, *346*, 818–822.
(13) Bock, L. C.; Griffin, L. C.; Latham, J. A.; Vermaas, E. H.; Toole, J. J. *Nature* **1992**, *355*, 564–566.
(14) Seelig, G.; Yurke, B.; Winfree, E. *J. Am. Chem. Soc.* **2006**, *128*, 12211–12220.
(15) Zhang, D. Y.; Turberfield, A. J.; Yurke, B.; Winfree, E. *Science* **2007**, *318*, 1121–1125.

Table 1. Sequences of DNA Strands Used in This Study[a]

strand name	sequence (5′→3′)
HCV (wild-type)	AGCCGAGTAGCGTTGGGTTGCGAAAGGCCTTGTGGTACTG
HCV† (T13A)	AGCCGAGTAGCGATGGGTTGCGAAAGGCCTTGTGGTACTG
HCV† (T13C)	AGCCGAGTAGCGCTGGGTTGCGAAAGGCCTTGTGGTACTG
HCV† (T13G)	AGCCGAGTAGCGGTGGGTTGCGAAAGGCCTTGTGGTACTG
HCV† (+A14)	AGCCGAGTAGCGTATGGGTTGCGAAAGGCCTTGTGGTACTG
HCV† (Δ13):	AGCCGAGTAGCGTGGGTTGCGAAAGGCCTTGTGGTACTG
avian flu (H5N1)	AGACCCAAAGTAAACGGGCAAAGTGGAAGAATGGAGTTCT
smallpox	GAAGCGTATTTCATGTGTAAGTTACAGGATCTAATTGTGA
displacement beacon top	(FAM)-ACTATGGGCGCA
displacement beacon bottom	CGTTTCATAGCAGCGCCAGATGCTGCGCCCATAGT-(dabcyl)
IDE inhibitor strand	(inhibitor)-TATGGGCGCAGC
IDE enzyme strand	CGTTTCATAGCAGCGCCAGATGCTGCGCCCATAGT-(enzyme)
intermediate	GCATCTGGCGCTGCTATGAAACGAGCCGAGTAGCGTTGGGTTGCGAAA
HCV (reverse complement)	(biotin)-CAGTACCACAAGGCCTTTCGCAACCCAACGCTACTCGGCT
output	ACTATGGGCGCAGCATCTGGCGCTGCTATGAAACG
intermediate (reverse complement)	TTTCGCAACCCAACGCTACTCGGCTCGTTTCATAGCAGCGCCAGATGC
HCV output*	ACTATGGGCGCAGCATCTGGCGCTGCTATGAAACGAGCCGAGTAGCGTTGGGTTGCGAAA
bird flu (reverse complement)	(biotin)-AGAACTCCATTCTTCCACTTTGCCCGTTTACTTTGGGTCT
bird flu output*	ACTATGGGCGCAGCATCTGGCGCTGCTATGAAACGAGACCCAAAGTAAACGGGCAAAGTG
smallpox (reverse complement)	(biotin)-TCACAATTAGATCCTGTAACTTACACATGAAATACGCTTC
smallpox output*	ACTATGGGCGCAGCATCTGGCGCTGCTATGAAACGGAAGCGTATTTCATGTGTAAGTTAC
adenosine aptamer	(biotin)-TCACTGACCTGGGGGAGTATTGCGGAGGAAGGTTTTTT
adenosine output*	CCCAGGTCAGTGACTATGGGCGCAGCATCTGGCGCTGCTATGAAACG

[a] FAM = fluorescein amidite. FAM, dabcyl, and biotin were appended using phosphoramidites or controlled pore glass supports obtained from Glen Research. See Figure 4 for details regarding inhibitor and enzyme portions of the IDE sequences. See Supporting Information for more detailed annotations of the binding domains.

targets,[16] it should be possible to produce translators of this type that can accept virtually any input molecule.

Materials and Methods

Diagnostic Sequences. All diagnostic sequences were selected to detect either viral genomic RNA or RNA transcripts to ensure that the targets would be available in single-strand form after sample preparation. Detection regions were selected to be within amplicon regions (often on the primer regions themselves) from established PCR diagnostics whenever available. Detection regions were also examined for folding characteristics in an effort to select regions likely to contain as little secondary structure as possible, with the exception of the HCV diagnostic sequence. The HCV sequence represents a worst-case scenario for folding, as it has been intentionally selected from a GC and secondary-structure-rich primer region. Hepatitis C virus diagnostic sequences are derived from hepatitis C virus strain (JFH-1) genomic RNA.[17] Sequences are located in regions that code for the HCV polyprotein (Genbank accession no. AB047639). The detection region (nt251−291) was selected from within the amplicon region, including the reverse primer for diagnostic RT-PCR. Avian influenza (H5N1) diagnostic sequences are derived from the (A/Hong Kong/156/97) strain.[18,19] Sequences are located in regions that code for the HA1/HA2 segments of hemeagglutinin (Genbank accession no. AF036356). The detection region (nt645−685) was selected from within the amplicon region for diagnostic PCR primers.[19] Smallpox virus diagnostic sequences are derived from the Variola major virus (Bangladesh-1975) strain.[20] Sequences are located in regions that code for the B9R transcript (Genbank accession no. L22579). The detection region (nt181−220) was selected from a region of minimal secondary structure within the diagnostic transcript. Human immunodeficiency virus (HIV) diagnostic sequences used in the inhibitor−DNA−enzyme (IDE) system are derived from the envelope glycoprotein transcript of HIV-1 isolate (Genbank accession no. EF514704).

DNA Purification, Synthesis, and Stock Preparation. All DNA strands were synthesized using an ABI model 394 DNA synthesizer with ultramild phosphoramidites, reagents, and controlled pore glass supports purchased from Glen Research (see Table 1 for DNA sequences). DNA was cleaved from the supports using mild cleavage conditions (concentrated ammonium hydroxide for 2−5 h at room temperature), purified via DMT-ON RP-HPLC on a Vydac C18 column using a binary gradient (solvent A, 0.1 M triethylammonium acetate, pH 7.5; solvent B, solvent A + 80% acetonitrile; gradient, 0−25% B over 30 min; flow rate, 3 mL/min), desalted with a Waters Sep-Pak Plus C18 column, and finally concentrated using a vacuum centrifuge. Stock solutions were prepared at 30 μM concentration in IDE buffer (50 mM $MgCl_2$, 20 mM Tris pH 7.4) using extinction coefficients at 260 nm calculated by the nearest-neighbor method via a web-based script (http://www.ambion.com/techlib/misc/oligo_calculator.html) and stored at 5 °C.

Displacement Beacon Preparation. Displacement beacons were prepared at a final concentration of 15 μM by mixing equal ratios of 30 μM stock solutions of the 5′-FAM-modified strand with the 3′-dabcyl-modified strand, heating to 85 °C for 5 min, and allowing the solution to come to ambient temperature over ∼6 h. Beacons were stored at 5 °C and allowed to equilibrate in quartz cuvettes by placing them in temperature-regulated (25 °C) cells for ∼15 min prior to usage.

Translator Preparation. Toe-hold sequestered translators (HCV → intermediate) and (intermediate → output) were prepared at 14.3 μM by mixing a slight excess of 30 μM complement strand with

(16) Shangguan, D.; Li, Y.; Tang, Z.; Cao, Z. C.; Chen, H. W.; Mallikaratchy, P.; Sefah, K.; Yang, C. J.; Tan, W *Proc. Natl. Acad. Sci. U.S.A.* **2006**, *103*, 11838–11843.

(17) Kato, T.; Furusaka, A.; Miyamoto, M.; Date, T.; Yasui, K.; Hiramoto, J.; Nagayama, K.; Tanaka, T.; Wakita, T. *J. Med. Virol.* **2001**, *64*, 334–339.

(18) (a) To, K. F.; Chan, P. K.; Chan, K. F.; Lee, W. K.; Lam, W. Y.; Wong, K. F.; Tang, N. L.; Tsang, D. N.; Sung, R. Y.; Buckley, T. A.; Tam, J. S.; Cheng, A. F. *J. Med. Virol.* **2001**, *63*, 242–246. (b) Yuen, K. Y.; Chan, P. K.; Peiris, M.; Tsang, D. N.; Que, T. L.; Shortridge, K. F.; Cheung, P. T.; To, W. K.; Ho, E. T.; Sung, R.; Cheng, A. F. *Lancet* **1998**, *351*, 467–471.

(19) Claas, E. C.; Osterhaus, A. D.; van Beek, R.; De Jong, J. C.; Rimmelzwaan, G. F.; Senne, D. A.; Krauss, S.; Shortridge, K. F.; Webster, R. G. *Lancet* **1998**, *351*, 472–477.

(20) Sofi Ibrahim, M.; Kulesh, D. A.; Saleh, S. S.; Damon, I. K.; Esposito, J. J.; Schmaljohn, A. L.; Jahrling, P. B. *J. Clin. Microbiol.* **2003**, *41*, 3835–3839.

30 μM output strand, heating to 85 °C for 5 min, and slowly (~6 h) cooling to ambient temperature and stored at 5 °C. Attempts were made to improve the performance (higher yield, lower background) of the hybrid translator complex by non-denaturing FPLC purification, but performance after purification was not substantially improved. Solid-phase translators (HCV → output*), (avian flu → output*), (smallpox → output*), and (adenosine → output*) were prepared at 7.5 μM by first annealing 1.1 equiv of 30 μM output* with 1.0 equiv of 30 μM biotinylated input complement strand at 85 °C for 5 min, followed by slowly (~6 h) cooling to ambient temperature. Streptavidin Sepharose high-performance beads (GE Healthcare, 34 μm mean particle size, highly cross-linked spherical agarose, loading minimum 300 nmol of biotin/mL of medium) were first washed five times with IDE buffer using Ultrafree-MC centrifugal 0.22 μm filters (Amicon Bioseparations). Next, an excess of the streptavidin Sepharose bead suspension was then incubated with the pre-annealed DNA (~100 equiv of streptavidin per biotinylated DNA gate complex) for 5 h with gentle shaking at room temperature. Finally, immobilized translators were washed (10 times) with ~3 volumes of IDE buffer to remove unbound output DNA and stored at 5 °C.

Beacon Fluorescence Assays. Fluorescence data were acquired on a Sim-Aminco Series 2 luminescence spectrometer with the AB2 (v5.5) software package (Thermo Electron). Each sample was excited at 494 nm (8 nm band-pass), with emission readings taken at 522 nm (8 nm band-pass), with a PMT sensitivity (gain) of 500 V. Beforehand, 6 μL of 15 μM beacon was allowed to pre-equilibrate in 3 mL of IDE buffer in a quartz cuvette at 25 °C.

For toe-hold sequestered translations, 3 μL of 30 μM input DNA or IDE buffer was incubated at room temperature with 6.3 μL of 14.29 μM (HCV → intermediate) for 5 min. Next, 6.3 μL of 14.29 μM (intermediate → output) was added and incubated at room temperature for another 5 min. The entire mixture was then injected into the cuvette, and emission recordings were taken with 1-s integration time for >1000 s. Ten-second running averages (averaged with pervious time points) were then applied to smooth the curve.

For solid-phase translations, 3 μL of 30 μM input or IDE buffer was incubated at room temperature with 40.9 μL of 6.6 μM (3 equiv) (HCV → output*) for 5 min. After incubation, the sample was centrifuged at ~1000 rpm briefly, and 10 μL aliquots of the supernatant were carefully removed and injected into the cuvette. Emission recordings were then taken with 1-s integration time for >1000 s. Thirty-second running averages (averaged with previous time points) were then applied to smooth the curve.

Single Nucleotide Polymorphism Analysis. An 18 μL slurry of ~7.5 μM solid-phase translator (HCV → output*), 3 μL of 30 μM HCV†, and 20 μL of IDE buffer was allowed to incubate at room temperature for various incubation times. After incubation, the sample was centrifuged at ~1000 rpm briefly, and 25 μL aliquots of the supernatant were carefully removed. Those aliquots were then injected into the cuvette, and emission recordings were taken with 1-s integration time for >1000 s. Ten-second running averages (averaged with forward time points) were then applied to smooth the curve.

Translation Yield Analysis. A 36 μL slurry of each ~7.5 μM solid-phase translator (HCV → output*), (avian flu → output*), (smallpox → output*) was incubated at room temperature with 3 μL of 30 μM input DNA (or buffer) for 5 min. After incubation, 20 μL of IDE buffer was added. The sample was mixed thoroughly, followed by centrifugation at ~1000 rpm briefly, and 25 μL aliquots of the supernatant were carefully removed. Those aliquots were then injected into the cuvette, and emission recordings were taken with 1-s integration time for >1000 s. Twenty-second running averages (averaged with forward time points) were then applied to smooth the curve.

IDE Coupled Translations. A 5 μL slurry of ~7.5 μM solid-phase translator (HCV → output*) was mixed with 1 μL of a solution with input concentrations ranging from 5 μM to 0.5 μM (5 pmol to 500 fmol). This mixture was allowed to sit at room temperature for 15 min, and then 24 μL of IDE buffer was added. This suspension was mixed thoroughly and centrifuged at ~3000*g* for 1 min to pellet the beads, and then 20 μL of the supernatant was carefully removed. Ten microliters of the translation output was then assayed using the IDE system.

IDE Assay. The DNA−inhibitor conjugate (5 μL, 400 nM) was mixed with the DNA−enzyme conjugate (5 μL, 40 nM) in buffer (50 mM $MgCl_2$, 20 mM Tris, pH 7.4) and incubated for 15 min. The translation output (10 μL, varying concentrations) was then added, and the mixture was incubated for another 15 min. Finally, the substrate (5 μL, 1.6 mM) was added and the mixture read in the plate reader. Fluorescence measurements were performed with a microplate reader (Genios, Tecan Instruments, $\lambda_{ex} = 365$ nm, $\lambda_{em} = 465$ nm) using black 96-well plates, with measurements taken every 60 s. Five-minute running averages (averaged with forward time points) were then applied to smooth the curve. Total reaction volumes of 100 μL were used in all enzyme reactions.

Multiplexing Plate Assay. The DNA−inhibitor conjugate (5 μL, 400 nM) was mixed with the DNA−enzyme conjugate (5 μL, 20 nM) in buffer (50 mM $MgCl_2$, 20 mM Tris, pH 7.4) and incubated for 15 min. The translation output (obtained as in IDE assays) was then added, and the mixture was incubated for another 15 min. Finally, the substrate (5 μL, 0.8 mM) was added and incubated for 20 min. The black clear-bottom 96-well plate containing these reactions was then illuminated from below at a wavelength of 302 nM. The visible fluorescence was observed with an Alpha Inotech gel imaging device and the contrast adjusted using Fluorochem imaging software (black, 7710; white, 10794; gamma, 1.2). Total reaction volumes of 100 μL were used in all enzymatic reactions.

HCV Genomic RNA Preparation. HCV genomic RNA was obtained using an Ambion MEGAscript translation kit (T7 version, catalog no. AM1334) and HCV JFH-1 genome under control of the T7 promoter.

Results and Discussion

Nucleic Acid Translation. Because the input and output of any DNA-to-DNA translation results in exceptionally similar observable properties (absorption spectra, mass, polarity, etc.), we required a sequence-specific method of detecting the output DNA in order to monitor and evaluate the results of the translation processes. For this purpose we opted to use a displacement beacon[21] with a toe-hold region that was carefully selected to match the sequestered portion of the output sequence (Figure 2A). With a means of quantitatively assaying translator output, we evaluated the behavior of a toe-hold sequestered translator that converted input sequences diagnostic of hepatitis C virus (HCV) infection to an output sequence detected by the beacon. We ascertained the yield of the second half-translator in the series (intermediate → output), the two coupled half-translations (HCV → intermediate → output), and the full translation background (output produced with no input) using the displacement beacon (Figure 2B). With 5 min incubations at room temperature, in low micromolar concentrations, the second half-translator produced 74% yield of the output (per intermediate input), and the full translation produced 53% yield of the output (per HCV input), which is roughly what one would expect given two coupled half-translations. When no input was present, the full translation background produced 13% of the full output signal. Background translation levels can originate from any unpaired excess of output and intermediate strands that remain after hybridization during the synthetic preparation

(21) (a) Li, Q.; Luan, G.; Guo, Q.; Liang, J. *Nucleic Acids Res.* **2002**, *30*, e5. (b) Shengqi, W.; Xiaohong, W.; Suhong, C.; Wei, G. *Anal. Biochem.* **2002**, *309*, 206–211.

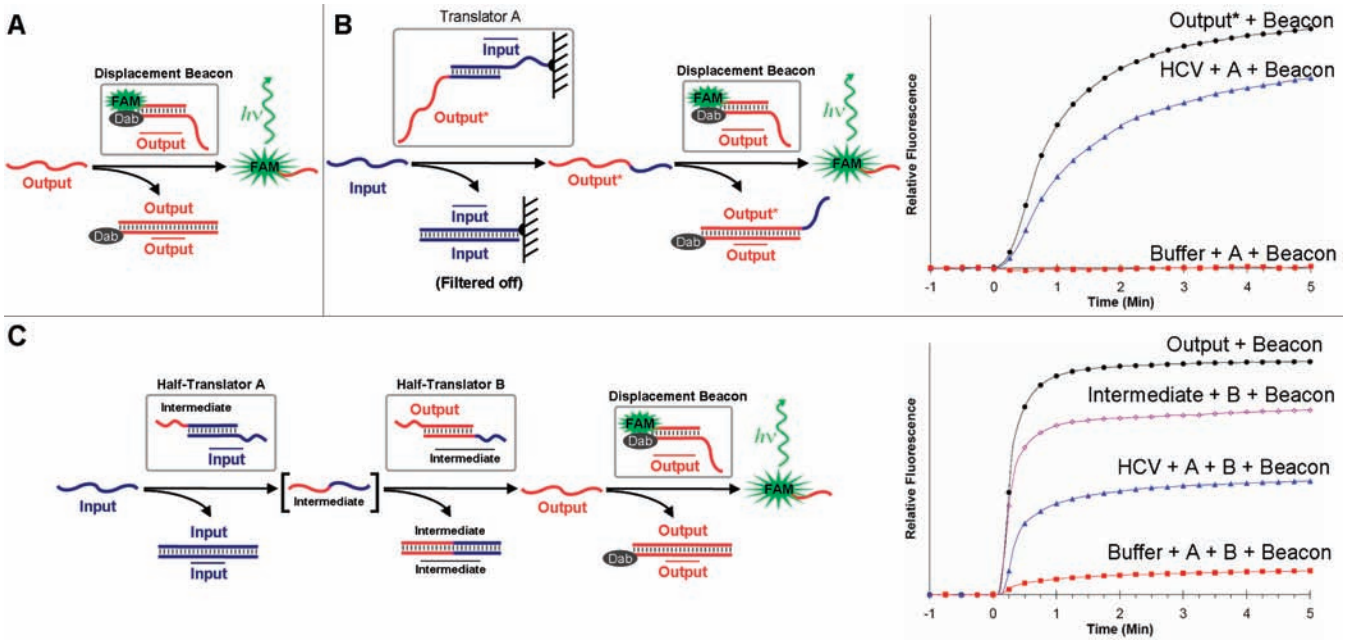

Figure 2. Displacement beacon-monitored translations of the hepatitis C virus (HCV) diagnostic input sequences. (A) Schematic of displacement beacon mechanism.[21] Translation output binds to the quencher-terminated strand (dabcyl, gray oval) and displaces the fluorophore (FAM, green star)-terminated strand into solution, thus freeing it from contact quenching and causing increased fluorescence emission. (B) Solid-phase translation of (HCV → output*), translation background (no input), and positive control of beacon spiked with translation output at the corresponding input levels. Experiments were performed with 36 μL of 7.5 μM translator (3 equiv) and 3 μL of 30 μM single-stranded DNA. Data are relative to the background fluorescence produced by the quenched beacon. (C) Toe-hold sequestered full translation (HCV → intermediate → output), partial translation (intermediate → output), full background (no input) of the translation, and a positive control of just the beacon spiked with output at the corresponding input levels. Experiments were performed with 6 μL of 15 μM translator, 6 μL of 15 μM beacon, and 3 μL of 30 μM single-stranded input DNA.

of the translator complex, as well as any single-stranded DNA released as a consequence of spontaneous melting of either duplex. Over time, this background leakage can integrate continuously to contribute to the background translation. Next we evaluated the behavior of a solid-phase translator that similarly converted HCV input DNA sequences to an output sequence detected by the beacon. With 5 min incubation times at room temperature, the solid-phase method resulted in a comparable 74% yield for positive translation (Figure 2C). Most strikingly, with this method the background levels were below the level of detection of the displacement beacon assay (<1%), even when a 3-fold excess of the translator was employed. The lower levels of background translation observed for the solid-phase architecture most likely result from the filtering event, which samples free strand produced by spontaneous melting at a single time point, as opposed to the toe-hold sequestered translators which integrate any spontaneous leakage continuously as time progresses. Additionally, in the case of the solid-phase translator there is only one translator duplex capable of contributing to background, whereas the toe-hold sequestered translators have two duplexes that can both contribute.

Distinguishing Single Nucleotide Polymorphisms. Encouraged by these results, we assessed the selectivity of solid-phase translation by comparing translation of the wild-type input (HCV) to a full panel of single nucleotide polymorphisms, including each point mutation variant, an insertion, and deletion mutation (Figure 3). Interestingly, nearest-neighbor calculated hybridization energies[22] of the mutant inputs to the immobilized strand are quite minimal (~5%). However, mismatches likely have a heightened transition-state barrier and corresponding slower kinetic rate during branch migration because the mutant must displace more than one base pair without being able to make a compensatory match at the site of mutation. We conducted translations with varying incubation times, postulating that with kinetically limiting incubation times discrimination should be optimal, and as each reaction approaches equilibrium our ability to resolve polymorphisms should degenerate to levels predicted by the final free energies. Not surprisingly then, at limiting incubation times (30 s), discrimination of the polymorphic DNA from the wild-type was excellent, but longer incubation times (1 or 5 min) led to losses in resolving ability (Figure 3B). Unexpectedly, the (T13C) mutant stood apart, displaying significantly enhanced discrimination compared to the other polymorphisms. After resynthesis of the (T13C) strand to confirm this observation, a closer examination indicated that the predictive folding energies[23] of each of the single-stranded mutants is within ~10% of the wild-type, with the exception of (T13C), whose free energy for folding is over 40% more stable than that of the wild-type (Supporting Information, Table S1). Thus, the T-to-C mutation affords a stable alternative secondary structure located throughout the toe-hold, which likely introduces a new rate-limiting step involving unfolding of this region (Supporting Information, Figure S3).

Application of Translators to Diagnostic High-Throughput Adaptation. With a sound fundamental understanding of the behavior of the solid-phase translators in hand, we set about interfacing them with IDE assay,[11] which is a high-gain isothermal nucleic acid detection system originally designed for HIV diagnosis (Figure 4A). Modifying the IDE detection sequence requires custom synthesis of the enzyme−DNA conjugate and involves lengthy synthetic steps, each requiring

(22) Markham, N. R.; Zuker, M. *Nucleic Acids Res.* **2005**, *33*, W577−581.

(23) Zuker, M. *Nucleic Acids Res.* **2003**, *31*, 3406–3415.

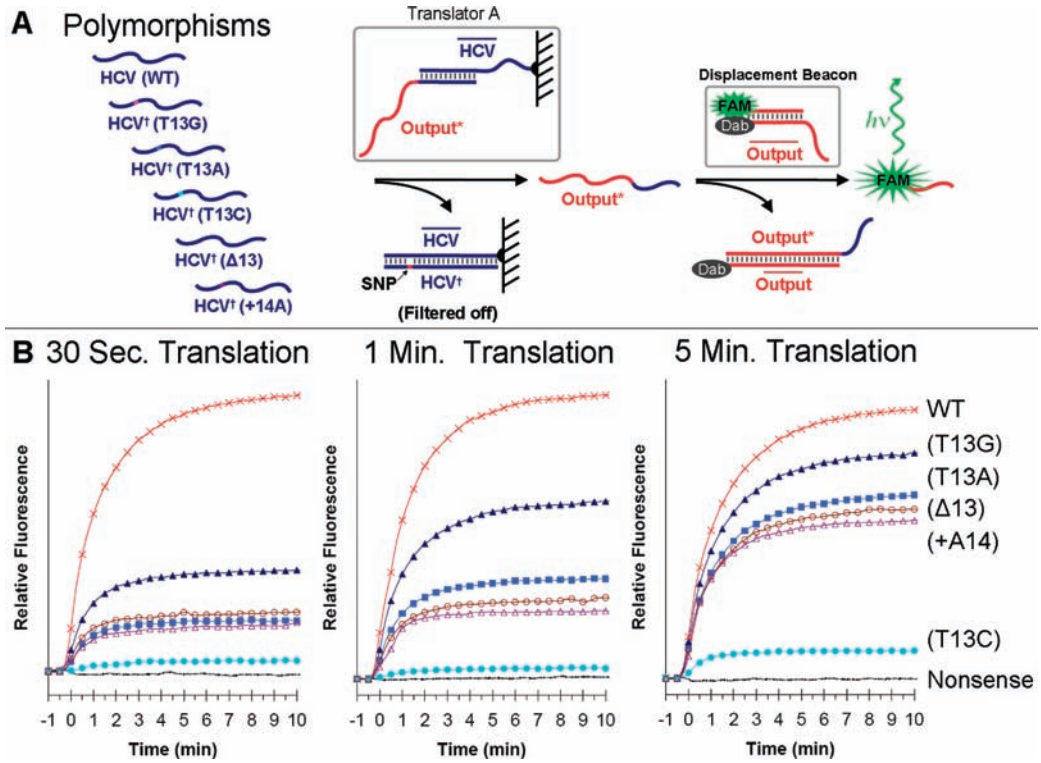

Figure 3. Solid-phase translation of HCV single nucleotide polymorphisms (SNPs). (A) Schematic of the translation reaction. The polymorphism is located on the input strand (HCV†) at roughly the center of the duplex region (13nt of 25bp) between the immobilized strand and the output. (B) SNP discrimination with increasing incubation time. The primary mechanism in discrimination of SNPs in this case is kinetic rather than thermodynamic. The SNPs must overcome a heightened transition-state barrier in order to displace the output, and therefore displacement proceeds more slowly. At limiting incubation times (30 s), discrimination of the SNP is excellent. However, as the reaction proceeds to equilibrium, the ability to resolve the SNPs deteriorates due to the minimal differences in final energies of each complex. Importantly, incubation of the translator with a nonsense sequence (dotted line) showed no response, again verifying that translation is indeed sequence specific. All experiments were performed with 3× translator (~7.5 μM) and single-stranded input DNA (~2.5 μM). Data are relative to the background fluorescence produced by the quenched beacon.

significant purification procedures and materials overhead. Thus, producing translators that output HIV diagnostic sequences would greatly aid in the practical application of this sensor. We started by first confirming that the IDE has a predictable high-gain, dose-dependent response to the HIV output sequence (Figure 4B) and no baseline sensitivity to the HCV input sequence (Figure 4C). However, when the HCV input was first incubated with solid-phase translator, the dose-dependent response was restored, and we were able to detect as little as 500 fmol of HCV diagnostic DNA (Figure 4D). The background translation was previously undetectable when employing displacement beacons. However, to maintain useful translation kinetics, an excess of translator was employed (7.5−75 equiv) when coupling to the IDE construct. Under these conditions, the high-gain IDE system was capable of establishing the background translation to be somewhere in the hundreds of femtomolar range. While one would expect lower translation background levels if fewer equivalents of translator were employed, it would come at the cost of slower detection kinetics.

Encouraged by the successful coupling of the IDE system with the solid-phase translator, we set out to demonstrate how the minimal overhead involved in producing these translators can allow for high-throughput adaptation of the IDE system. Using just two commercially available oligomers per input, we produced two more solid-phase translators for diagnostically interesting sequences: avian influenza (H5N1) and smallpox virus. A quick comparison of translation yields using the aforementioned displacement beacon assay revealed positive yields (avian flu = 96% and smallpox = 75%) similar to those obtained with the HCV solid-phase translator (74%) while maintaining an undetectably low (<1%) background level with 5 min, room temperature, low micromolar translations (Figure 5A). Next, in a 96-well plate we arrayed each of the solid-phase translators in one dimension and each of the input sequences in the other. We then added identical IDE components to each of the wells and photographed the plate under fluorescent excitation (Figure 5B). This experiment clearly demonstrated that the IDE was activated only in wells where the input matched its cognate translator. Finally, in order to demonstrate the real-world feasibility of solid-phase translation, we translated genomic RNA from HCV into output DNA at levels detectable by the IDE assay (Supporting Information, Figure S2A). We found that 10 μg (~3 pmol) at 5 μg/μL (~1.5 μM) of whole genome HCV RNA was readily detectable after isothermal translation, despite the potentially increased difficulty of dealing with more heavily structured and chemically labile input (Supporting Information, Figure S2B).

Small-Molecule Translation. We next went on to explore a general strategy utilizing aptamers,[12,24] in which the molecular target of the aptamer and the output DNA compete for binding to the imm obilized aptamer (Figures 2D and 6). Although detection assays based on exploiting the competitive equilibrium between DNA binding and aptamer target binding have been previously explored,[25] to our knowledge such equilibria have not been previously employed in molecular translation schemes.

(24) Wilson, D. S.; Szostak, J. W. *Annu. Rev. Biochem.* **1999**, *68*, 611–647.

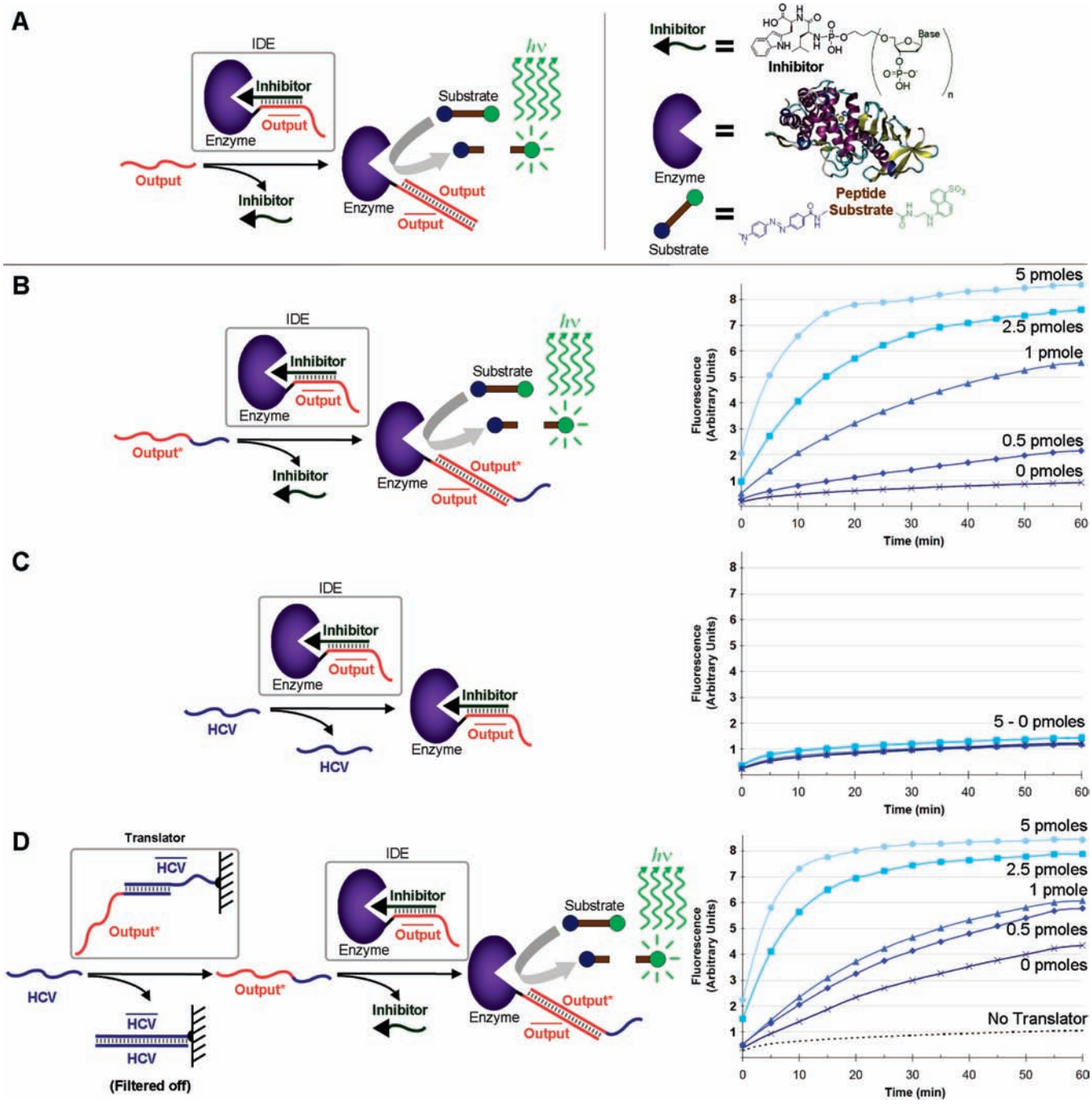

Figure 4. Translation coupled to a highly sensitive detection assay. (A) Schematic of the previously described[11] inhibitor−DNA−enzyme (IDE) system. The IDE system is composed of a mutant form (E151C) of the enzyme cereus neutral protease (CNP, shaded purple oval) with a DNA strand (output-Bar, light red) covalently attached to the mutated residue via a disulfide positioned near the active site of the protease (PDB ID 1NCP). Next, a partial cDNA strand (dark green) with a covalently attached protease inhibitor (noncleavable substrate mimic, black triangle) on its 5′ end is allowed to hybridize with the DNA−enzyme construct. This templated inhibition of the enzyme curtails the majority of the enzyme activity using only a few fold excess of inhibitor−DNA. Addition of an HIV diagnostic detection sequence (output, red), initiates irreversible strand displacement, removing the inhibitor's supramolecular anchoring to the enzyme and restoring the majority of the activity.[11] Enzymatic activity is monitored via a fluorogenic peptide substrate (dabcyl-βAla-Ala-Gly-Leu-Ala-βAla-EDANS) that can be enzymatically cleaved by the protease, thereby freeing the EDANS fluorophore from the dabcyl quencher and generating a fluorescent signal. (B) (HCV → output*) solid-phase translation coupled to IDE. Varying quantities of input are labeled from light blue to dark blue. The enzyme shows a clear dose-dependent response to the output* strand. (C) Input = HCV, no translator. Enzyme activity drops to baseline and all dosage information is lost, demonstrating that the IDE construct is unaffected by the HCV input. (D) Input = HCV, with 15 min incubation of ~30 pmol of (HCV → output*) solid-phase translator. Enzyme activity is restored as HCV is translated in a dose-dependent manner into output*. A negative control consisting of only the IDE construct and substrate (black dotted line) reveals the expected baseline of the IDE system if no output* is present. When coupled to the high-gain IDE assay, the previously undetectable background translation (via displacement beacon assay) reveals itself to be somewhere in the hundreds of femtomoles range.

Moreover, it is important to underscore the fundamental differences between the mechanism by which the nucleic acid translators and the aptameric translators function. In the case of the nucleic acid translators, the input has a longer stretch of complementarity to the immobilized strand than the output, causing translation to be thermodynamically downhill. In

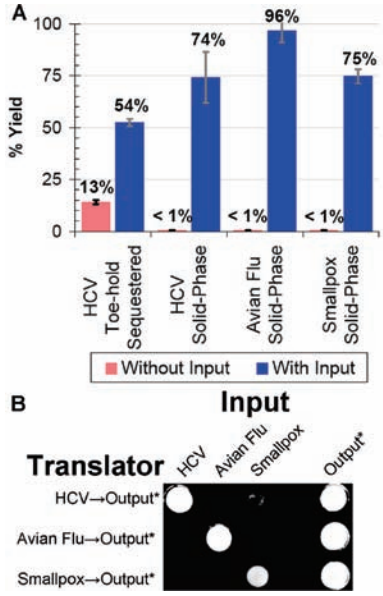

Figure 5. Analysis of translation yield and high-throughput adaptation of high-value diagnostic targets. (A) Comparison of several translations and their associated yields. Translations were performed with 5 min incubation at room temperature with low micromolar concentrations. Translation yields were then determined by comparing the fluorescence generated by the beacon when incubated with a reference sample of pure translation output and with the results of each 5 min translation (with and without the inputs present). The blue bars represent translations in the presence of the input, while red bars represent translation background with no input present. Error bars represent ±1 SD from a set of three consecutive translations. For all three solid-phase translators, the background translation was below the level of detection (<1%). Variation in yields can probably be ascribed to factors such as secondary structure of the input sequences (for which the avian influenza sequence is predicted[23] to have very little), varying purity in DNA preparation, and pipetting error. (B) Photograph of a portion of a 96-well plate under UV illumination (302 nm), demonstrating the capability of these solid-phase translators to adapt distinct assays for high-throughput analysis. Each of the three solid-phase translators, (HCV → output*), (avian flu → output*), and (smallpox → output*), were arrayed in rows, incubated with each of their three inputs (HCV, avian flu, and smallpox) arrayed in columns, and assayed using the IDE detection system. Additionally, a column of positive controls was included (output*), which is incidentally indicative of HIV diagnostic detection. Experiments were performed with 5 μL of translators (7.5 μM) and 2 μL of input DNA (5 μM).

addition, kinetic barriers are minimal due to the available branch migration mechanism, which allows for spontaneous displacement at room temperature. In contrast, free energies for small-molecule binding to aptamers are generally much smaller than for binding a complementary nucleic acid, and therefore it is likely that this type of translation will be thermodynamically uphill. Additionally, any mechanism closely resembling branch migration is unlikely to be available, given that aptamers are usually selected solely for their ability to bind the target. Finally, aptamers tend to depend upon well-defined secondary structures that would likely preclude any simultaneous duplexation with the output. Thus, it is likely that the competitive binding of the molecular input and the output DNA with the aptamer will more closely resemble a two-state mechanism, requiring a full dissociation of one binding partner before another can replace it. With this in mind, care must be taken to design appropriately sized complementary output DNA strands and operate with an excess of the molecular input to shift the equilibrium in favor of output strand dissociation. Additionally, should kinetic barriers pose time constraint issues, the translator can simply be annealed in the presence of the input molecule to allow the system to proceed quickly to its thermodynamic minimum. A proof-of-principle aptameric solid-phase translator as described was constructed using an adenosine aptamer[26] and was coupled to the IDE assay (Figure 6A). After the translator was applied, the IDE showed a dose-dependent response to the adenosine input (Figure 6B), demonstrating the feasibility of translating a small-molecule input into a desired sequence-specific output DNA. However, the relatively low affinity of the aptamer for adenosine required us to use high concentrations (millimolar) of the input to effect the translation.

Theoretical Basis

For rational engineering of effective aptameric translators, it is important to derive competitive equilibrium expressions to better understand and predict system behavior. If we define [translator] as the output DNA aptamer hybrid, then the equilibrium expression describing the background dissociation is given by

$$\text{translator} \overset{K_{\text{D out}}}{\rightleftharpoons} \text{aptamer} + \text{output}$$

We can therefore derive expressions for the equilibrium concentration of background output as a function of initial translator concentration and the dissociation constant of the output DNA to the aptamer DNA ($K_{\text{D out}}$) using standard equilibrium expressions and conservation of mass as described by eq 1 (derivation in Supporting Information):

$$[\text{output}] = -\frac{1}{2}K_{\text{D out}} + \frac{1}{2}\sqrt{K_{\text{D out}}^2 + 4K_{\text{D out}}[\text{translator}]_0} \quad (1)$$

Now consider the case where the input molecule is introduced into the system. Given a two-state competitive binding mechanism, when in the presence of input molecule, a competitive equilibrium is established whereby

$$\text{translator} \overset{K_{\text{D out}}}{\rightleftharpoons} \text{aptamer} + \text{output}$$

$$\text{waste} \overset{K_{\text{D in}}}{\rightleftharpoons} \text{aptamer} + \text{input}$$

The exact expression for the equilibrium concentration of output produced as a function of initial translator concentration, initial concentration of the input molecule, and the dissociation constants of the aptamer ($K_{\text{D in}}$) and the DNA duplex ($K_{\text{D out}}$) is given by eq 2[27] (derivation in Supporting Information).

$$[\text{output}] = [\text{translator}]_0 - \frac{[\text{translator}]_0(2\sqrt{\alpha^2 - 3\beta}\cos(\theta/3) - \alpha)}{3K_{\text{D out}} + (2\sqrt{\alpha^2 - 3\beta}\cos(\theta/3) - \alpha)} \quad (2)$$

where

(25) (a) Dirks, R. M.; Pierce, N. A. *Proc. Natl. Acad. Sci. U.S.A.* **2004**, *101*, 15275–15278. (b) Nutiu, R.; Li, Y. *Angew. Chem., Int. Ed.* **2005**, *44*, 5464–5467. (c) Zayats, M.; Huang, Y.; Gill, R.; Ma, C.-a.; Willner, I. *J. Am. Chem. Soc.* **2006**, *128*, 13666–13667. (d) Yoshida, W.; Yokobayashi, Y. *Chem. Commun.* **2007**, 195–197. (e) Wei, B.; Cheng, I.; Luo, K. Q.; Mi, Y. *Angew. Chem., Int. Ed.* **2008**, *47*, 331–223.

(26) Huizenga, D. E.; Szostak, J. W. *Biochemistry* **1995**, *34*, 656–665.
(27) Wang, Z. X. *FEBS Lett.* **1995**, *360*, 111–114.

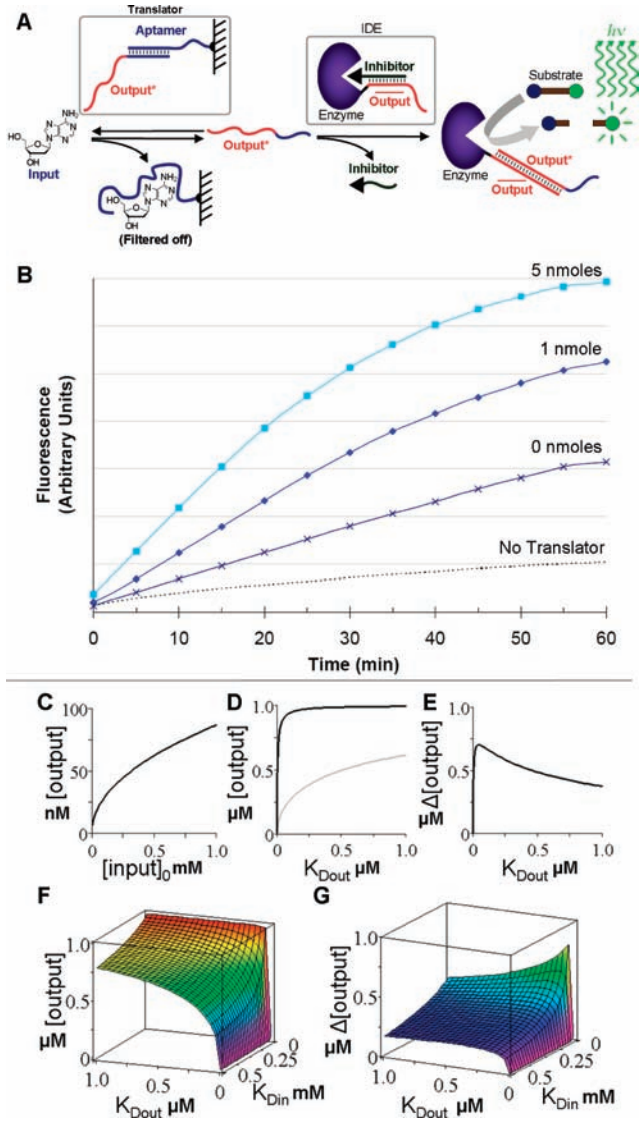

Figure 6. Solid-phase translation of small-molecule adenosine input into output DNA capable of triggering the IDE construct and plots of the equilibrium expressions describing its function. (A) Schematic of (adenosine → output*) translation utilizing a previously described[26] adenosine binding aptamer. (B) Dose-dependent response of the translation under varying amounts of adenosine input and a negative control depicting the background florescence produced by the IDE system (black dotted line). (C) Equilibrium expression depicting expected output with varying $[input]_0$, exhibiting a nonlinear behavior over large variations in input concentration (0−1 mM) but approximately linear at the high end (0.5−1 mM). When not specified by the axis, the parameters employed were as follows: $[translator]_0 = 1\ \mu M$, $[input]_0 = 1$ mM, $K_{D\,out} = 50$ pM, and $K_{D\,in} = K_{D\,adenosine} = 6\ \mu M$. (D) Positive translation (black) and background (gray) output levels with varying $K_{D\,out}$. The $K_{D\,out}$ can be varied by modifying the length of the duplex anchoring the output to the aptamer. As the duplex gets smaller, the affinity gets lower, the dissociation constant increases, and both the positive translation output (black) and the background output (gray) increase. However, at an excess of $[input]_0$, positive translation levels increase more rapidly with increasing $K_{D\,out}$ than background levels until the foreground level exhausts any available translator and output levels plateau. (E) Δ[output] (positive translation less background) with varying $K_{D\,out}$. By examining the separation between foreground (positive translation) and background output levels, we can clearly see that there is a local maximum in the separation just before the foreground levels begin to plateau. (F) Output levels with varying $K_{D\,out}$ and $K_{D\,in}$. Although there is a complex dependence, in general the higher the affinity of the aptamer for the input (lower, $K_{D\,in}$) and the lower the affinity of the aptamer for the output (higher $K_{D\,out}$), the more output is produced. (G) Δ[output] (positive translation less background) with varying $K_{D\,out}$ and $K_{D\,in}$, demonstrating that increases in output affinity (decreases in $K_{D\,out}$) are productive until a steep dropoff as the affinity becomes too great to displace the output. This dependence gets more pronounced, in a nonlinear fashion, as affinity for the input increases (decrease in $K_{D\,in}$).

$$\theta = \arccos\frac{-2\alpha^3 + 9\alpha\beta - 27\gamma}{2\sqrt{(\alpha^2 - 3\beta)^3}}$$

$$\alpha = K_{D\,out} + K_{D\,in} + [input]_0$$

$$\beta = K_{D\,out}([input]_0 - [translator]_0) + K_{D\,out}K_{D\,in}$$

$$\gamma = -K_{D\,out}K_{D\,in}[translator]_0$$

Equations 1 and 2 allow us to determine the respective foreground and background of aptamer-assisted translation, given reliable dissociation constants for the aptamer−input complex ($K_{D\,in}$) and the aptamer−output duplex ($K_{D\,out}$). It is important to note that the derived expressions represent lower bounds, as they assume that all of the output DNA is initially bound in the translator complex. Additionally, the assumption that each unique aptamer operates with a two-state competitive binding mechanism may or may not be valid in every circumstance. With those points in mind, the above model should provide a useful guide for rational engineering of aptameric translators.

When attempting to estimate input quantities on the basis of quantitative data regarding the output of a translation, we can simply examine the [output] vs $[input]_0$ in eq 2 (Figure 6C). To address an important design question regarding choosing a length for the output−aptamer duplex, we can plot the output of the positive translation (with 1 mM input, for example) and the background (no input) with varying affinity of the duplex ($K_{D\,out}$) (Figure 6D). Closer examination of the Δ[output] (positive translation less the background) with varying $K_{D\,out}$ reveals a clearly defined local maximum that establishes the values for which separation between the background and foreground signals is optimal (Figure 6E). In addition to optimizing for Δ[output], it can be useful in some situations to find parameters that lead to output values in the dynamic range of whatever assay to which one wishes to couple the output. For instance, the high-gain IDE system places strict demands on the background (<10 nM), and thus a $K_{D\,out}$ of ∼50 pM was required to obtain a low enough background while maintaining a clearly defined positive translation single. Given that the K_D of an aptamer could vary significantly from our example (adenosine, ∼6 μM), it is instructive to examine the behavior of the system with varying $K_{D\,in}$ values. If we vary $K_{D\,in}$ in one dimension and $K_{D\,out}$ in the other and plot the positive translation output (Figure 6F) or the Δ[output] (Figure 6G) on the *Z*-axis, we can anticipate the expected output given a set of affinities. It is also worth noting that $K_{D\,out}$ values that lead to minimal Δ[output] vary with $K_{D\,in}$, and thus duplex anchor lengths must be customized in accordance with the affinity of the aptamer for its target to obtain these maxima.

Conclusions

The ability to chemically translate any input molecular information into a readily processed output would be invaluable for rational engineering of advanced biomedical and diagnostic systems. With the simple translator constructs and components described, any sequence-specific assay can be universally applied to a new target without the need to modify the underlying technique. The minimal overhead involved in both the construction and operation of these translators also makes high-throughput adaptation feasible in cases where modifying the detection assay is too costly or time-consuming to pursue. Additionally, we have introduced molecular targets unrelated

to nucleic acids into the realm of potential inputs for translation via aptamers, which should allow for label-free detection of any analyte an aptamer can recognize. A proof-of-principle translation of this type, along with the thorough mathematic description of the system described here, should greatly facilitate routine engineering of these types of translators. We expect that such versatile translation strategies will open new and exciting possibilities in chemical and biomedical diagnostics. We also speculate that the ability to interface functionally unrelated molecular techniques and components with nucleic acid circuitry capable of both logical[8,9] and quantitative[8,15,28] processing might one day allow for modular programming and automated implementation of a vast array of powerful techniques entirely *in vitro*, without the need for persistent intervention from skilled personnel.

Acknowledgment. We thank our colleagues N. Gianneschi, L. J. Leman, and J. Chu for many helpful discussions and Stefan Wieland of The Scripps Research Institute for providing us with genomic RNA preparation. This research was funded in part by The Skaggs Institute for Chemical Biology.

Supporting Information Available: Supporting figures, mathematical derivations, DNA sequences, and further experimental methods involving IDE preparation. This material is available free of charge via the Internet at http://pubs.acs.org.

JA902490X

(28) Yin, P.; Choi, H. M. T.; Calvert, C. R.; Pierce, N. A. *Nature* **2008**, *451*, 318–322.